JREE: Vol. 9, No. 1, (Winter 2022) 93-105

Journal of Renewable Energy and Environment

Journal Homepage: www.jree.ir

Materials and Energy Research Center

MERC

Research Article

Chlorella vulgaris Cultivation Using Triangular External Loop Airlift Photobioreactor: Hydrodynamic and Mass Transfer Studies

Shiva Shadpour [a], Ali Pirouzi [a*], Mohsen Nosrati [b], Hoda Hamze [c]

[a] *Department of Chemical Engineering, University of Science and Technology of Mazandaran, P. O. Box: 48518-78195, Behshahr, Mazandaran, Iran.*
[b] *Biotechnology Group, Faculty of Chemical Engineering, Tarbiat Modares University, P. O. Box: 14115-143, Tehran, Tehran, Iran.*
[c] *Chemistry and Chemical Engineering Research Center of Iran (CCERCI), P. O. Box: 14335-186, Tehran, Tehran, Iran.*

PAPER INFO

Paper history:
Received: 13 June 2021
Revised in revised form: 04 August 2021
Scientific Accepted: 10 August 2021
Published: 08 January 2022

Keywords:
Airlift Photobioreactor,
Chlorella vulgaris,
Hydrodynamics,
Mass Transfer,
Mixing Time

ABSTRACT

Long mixing time, high power consumption, and small mass transfer coefficients are common problems in the photobioreactor design for microalgae culture which have a great effect on system efficiency and performance, CO_2 stabilization, and biomass production. In this study, a special design of the triangular external loop airlift photobioreactor was studied. The bioreactor's geometry was such that the angle between hypotenuse and the horizontal side (α) could vary. This configuration created an effective gas-liquid countercurrent flow in the downcomer section. In the present research, hydrodynamic and mass transfer of the reactor were investigated on the microalgae productivity under different design and operating parameters. The optimum conditions for the enhancement of *Chlorella vulgaris* productivity were explored by analyzing the mixing time (t_m), volumetric power consumption (P/V), mass transfer coefficients (k_La), bubble diameter (d), and gas holdup (ε) as responses. The results showed that the hypotenuse angle of $\alpha = 59^o$ and the superficial gas velocities of the V_{gs1} = 0.0050 m.s^{-1} for the downcomer and V_{gs2} = 0.008 m.s^{-1} for the riser of the reactor were the best conditions to achieve the highest biomass productivity. The responses' values obtained in the optimum condition were as follows: k_La_R= 19.67 (h^{-1}), k_La_D = 23.79 (h^{-1}), k_La_S = 23.76 (h^{-1}), $\theta_m = t_m/t_c$= 0.41, and P/V = 62.83 W/m^3, which had a smaller deviation than the actual values. The highest concentration of *Chlorella vulgaris* (X_{max} = 1.4 g.l^{-1}) achieved in this work was obtained in a shorter span of time (11th day of cultivation) based on the growth curve in optimized conditions.

https://doi.org/10.30501/jree.2021.290449.1216

1. INTRODUCTION

A photobioreactor (PBR) is specialized equipment designed to cultivate photosynthesis microorganisms such as microalgae species and operates under optimal light, mixing time, and mass transfer [1]. This equipment provides the ability to produce pure microalgae from CO_2 (free of any contamination) [2]. Airlift photobioreactor and bubble columns are systems in which the mixing of the fluids is performed by the gas bubbles created by the sparger placed at the base of the column [3]. An external-loop airlift PBR is one kind of the bubble-column that provides more favorable culture conditions by making a proper mixing process through the liquid phase circulating [4]. In these photobioreactors, lower turbulence is observed than the bubble column because of the adjustment of the vortexes by the bubble formation [5]. Also, due to the mixing improvement at the external-loop airlift PBR, a more homogenous environment for microalgae culture is provided [6, 7].

*Corresponding Author's Email: a.pirouzi@mazust.ac.ir (A. Pirouzi)
URL: https://www.jree.ir/article_143018.html

Nonetheless, the economic feasibility of microalgae production in these devices is significantly affected by cultivation technology and process designing [8]. It has been proven that the microorganism growth rate is dependent on the mixing process. However, the mobility of the culture medium (either mechanically or by aeration) along severe tensions can influence the growth rate negatively, which consequently made the biomass separation difficult [9]. In addition, it is expected that the superficial gas velocities could be effective in the mixing, CO_2 adsorption, and availability of the light and nutrient in the culture system. The previous research carried out by Powtongsook et al. (2006) [10] has shown the influence of varying superficial gas velocities on the growth of *H. pluvialis* cells in an airlift PBR. They have reported that the main reason for growth decline is the increased shear stress due to high sparging rates [10]. Also, other research studies have proven morphological damages to the microorganisms due to the hydrodynamic tensions [11].

Besides, it is now well established that the microalgae growth is controlled by the mass transfer of CO_2 from gas to liquid phase [12]. CO_2 diffusion from the gas phase to the mass bulk is related to the overall mass transfer coefficient

Please cite this article as: Shadpour, Sh., Pirouzi, A., Nosrati, M. and Hamze, H., "*Chlorella vulgaris* cultivation using triangular external loop airlift photobioreactor: Hydrodynamic and mass transfer studies", ***Journal of Renewable Energy and Environment (JREE)***, Vol. 9, No. 1, (2022), 93-105. (https://doi.org/10.30501/jree.2021.290449.1216).

(k_La), which itself is influenced by the bubble size, mixing rate, and the superficial gas velocity through the media [13]. Several works have been conducted to formulate the mass transfer and seek the best condition in gas-liquid systems [13-15]. It is very significant to consider that good mixing should be achieved with the least power usage. According to the investigations, mixing time decreases with increasing aeration rates. Also, the volume of the photobioreactor and its geometry influence the mixing time [16]. Moreover, the mixing time in the airlift PBRs increases significantly with the addition of the riser height.

Additionally, the gas holdup as an essential factor in photobioreactor design and its scale-up are associated with the superficial gas velocity, fluid circulation rate, the nozzle type, and the gas bubble sparger [17-19]. With the increment of gas feeding, the gas holdup of the bioreactor is reduced. For example, based on previous studies, more gas holdup implies a longer mixing time and higher mass transfer coefficients in the bioreactors [19]. It is not an absolute principle and can be changed by the photobioreactors' geometry and arrangement and, consequently, by the gas flow regime [19, 20].

Therefore, process optimization and improvement of biomass productivity require studying hydrodynamics and mass transfer of culture mediums. According to the reports, despite the high energy demand of photobioreactors, the biomass produced is very low. An innovative design of a photobioreactor can result in high microalgae growth rates and lower production costs [21]. Due to their many advantages, the airlift photobioreactors, including their high compatibility with three-phase media, lack of stirring equipment, and proper mixing, compared to the stirred tank and the type of bubble column, provide a suitable environment for biotechnology processes [22]. In these bioreactors, a regular stream is generated through the system using aeration principles to prevent shear stresses. Through the feeding of carbon dioxide-rich air, the mixing process and CO_2 supply in such systems are provided [23]. The mixing intensity, hydrodynamic, and mass transfer properties are critical design parameters of the bioreactors [20, 23].

In this study, the specific case of a triangular external loop airlift photobioreactor has been studied to cultivate *Chlorella vulgaris*. In earlier photobioreactors, the downcomer have demonstrated poor mass transfer and gas hold-up, which limits the residence time of air bubbles in this section of photobioreactors. In the present study, the creation of a countercurrent flow and high vortices in the downcomer increased the performance of the mixing and mass transfer process. This work aimed to investigate the influences of the geometry and operational parameters on the system performance. We evaluated how superficial gas velocities can influence the hydrodynamic and mass transfer behavior. This research set out to understand the effect of another critical factor better, the angle between the hypotenuse (downcomer) and the bioreactor's horizontal side (α). Response Surface Methodology (RSM) combined with the Central Composite Design (CCD) was applied to data analysis.

2. EXPERIMENTAL

2.1. Photobioreactor

Plexiglass-made triangular external loop photobioreactor with a working volume of 63 l was utilized for the research. A schematic diagram of the experimental setup is presented in Figure 1. The PBR includes two main sections: the upstream tube (riser) and the external loop, connected to the reactor from the top at an angle of 45° acting as the downcomer. The bioreactor's geometry is such that the angle between hypotenuse and the horizontal side (α) can vary. In this system, the gas was sparged from two locations: the lowest point of the hypotenuse and the riser. So, the gas and liquid were contacted co-current and countercurrent at the riser and downcomer, respectively. The mixing rate created in this way depends on the bioreactor's shape and geometry and superficial gas velocities. The superficial gas velocities of the downcomer and riser were denoted by V_{gs1} and V_{gs2}, respectively. All tests were performed at 25 °C and controlled using a computer Temperature Loop Controller (TLC), and a heat exchanger. The pH was adjusted by sodium hydroxide (1 M) and hydrochloric acid (1 M) solutions through two metering pumps controlled by the computer.

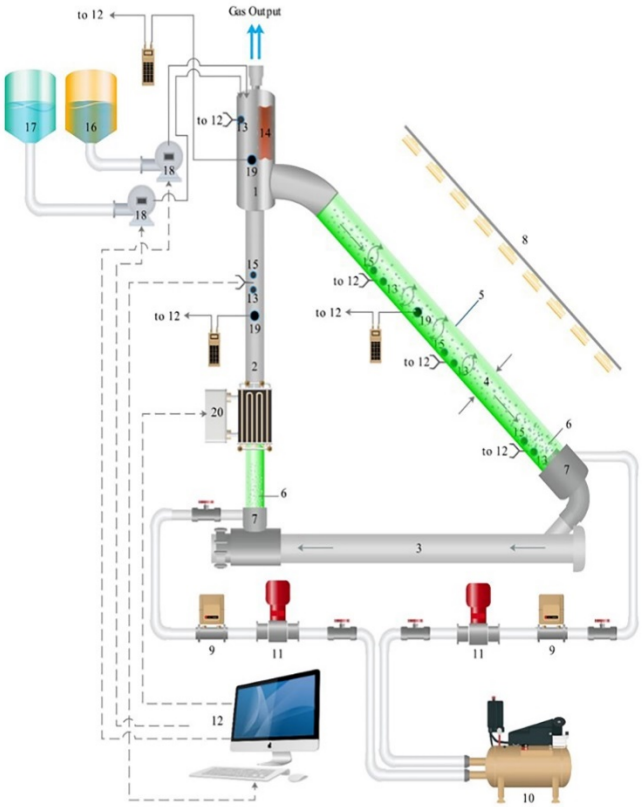

Figure 1. Schematic of an external airlift loop PBR. 1: Separator; 2: Riser; 3: Horizontal side; 4: Diameter of hypotenuse; 5: Downcomer; 6: Bubble; 7: Bubble sparger; 8: Light source; 9: Digital gas flow meter; 10: Compressor; 11: Gas sterilizer, filter; 12: PC; 13: Thermometer; 14: Heater; 15: pH probe; 16: NaOH solution; 17: HCl solution; 18: Dozing pump; 19: DO sensor; 20: Heat exchanger

3. METHOD

3.1. *Chlorella vulgaris* cultivation

The strain *Chlorella vulgaris* (ISC23) was provided from microalgae bank at Shahid Beheshti University, Tehran, Iran. The culture medium (N8) used in this study contained the following components: $Na_2HPO_4.2H_2O$ (0.260 g/l)), $MgSO_4.7H_2O$ (0.050 g/l), KH_2PO_4 (0.232 g/l), $CaCl_2.6H_2O$ (0.010 g/l), KNO_3 (1.000 g/l), Fe-EDTA (0.010 g/l), and trace elements solution of 1 ml. The trace elements mixture was made by the following constituents: $Al_2(SO_4)_3$ (3.580 g/l), $MnCl_2.4H_2O$ (12.980 g/l), $ZnSO_4.7H_2O$ (1.830 g/l), and

$CuSO_4.5H_2O$ (3.200 g/l). The pH of the medium was adjusted in the range of 6.8-7.0. The tap water was used for all experimental runs, and the required CO_2 was supplied through aeration.

3.2. Measurements

Liquid mixing is one of the essential factors that should be considered in the design and operational conditions. Good mixing in the bioreactor leads to minimizing the nutrient's transmission period into biomass during the culture. Here, mixing time (t_m) is characterized by the time needed to obtain 95 % complete mixing through the system [16]. This time is calculated by the acid trace technique [24]. Circulation time (t_c) and superficial fluid velocity were estimated by this method. The time needed for the flow to thoroughly loop around the reactor is specified by the circulation time and determined by the time period between the two pH consecutive peaks. The overall liquid velocity was calculated by dividing the tracer's travelled length by the circulation time [25]. The proportion of the airflow rate (Q) and each section's cross-sectional area was calculated as the superficial gas velocity (V_{gs}) of the section [26].

The overall gas holdup (ε) as a function of volume expansion to the initial volume (un-aerated volume) was measured using a volume expansion technique [27]. The volume expansion of a region of the reactor is defined as a differential hydrostatic pressure of two heads of that region. A U-tube inverted differential manometer measured the pressure difference.

The liquid phase's volumetric mass transfer coefficient (k_La) was estimated by the dynamic gassing out measurements [19]. In this method, Dissolved Oxygen (DO) was withdrawn from the liquid phase by injecting N_2 gas. Since the O_2 removal was completed, the air was introduced and the increase in dissolved O_2 concentration was recorded with time by a DO electrode. The following expression determined mass balance for oxygen:

$$\frac{dC}{dt} = k_La(C^* - C) \quad (1)$$

where C and C^* denote the dissolved O_2 concentration and the saturated one, and t points to the time.

The power per unit volume (P/V) referred to the volumetric power consumption as described by the following equation [16, 28]:

$$\frac{P}{V} = \frac{\rho_L \times g \times (A_D V_{gs1} + A_R V_{gs2})}{A_D + A_R} \quad (2)$$

where A_R and A_d are the cross-sectional areas of the riser and downcomer sections, respectively, ρ_L is the liquid density, and g is the gravitational acceleration.

3.3. Experimental design

The studies are focused on three parts of the downcomer (the hypotenuse), riser (the vertical side), and gas-liquid separator of this system. The effects of three main independent factors including superficial gas velocities inside the riser (V_{gs2}), the downcomer (V_{gs1}), and the angle (α) are investigated on the hydrodynamic and mass transfer performance. In order to optimize the mentioned factors, the RSM with combined CCD has been used. The upper and lower limits of the variables were obtained by performing preliminary tests. The parameters range and level are presented in Table 1. If gas feeding rates are higher than the limits, it leads to liquid overflow from the upper tube of the separator. Also, given the geometry of the PBR, there is no possibility of changing the angle out of the mentioned range. Based on these three main variables and their limitations, twenty experiments were designed and carried out. The quantities of mass transfer coefficients (k_La), gas holdup (ε), mixing time (t_m), fluid circulation time (t_c), bubble diameter (d), and volumetric power (P/V) have been measured as responses. The results were analyzed by the Design-Expert software version 7 (Stat-Ease Inc., Silicon Valley, CA, USA) based on the second-order model as follows:

$$Y = \beta_0 + \sum_{i=1}^{3} \beta_i x_i + \sum_{i=1}^{3} \beta_{ii} x_i^2 + \sum_{i=1}^{2} \sum_{j=i+1}^{3} \beta_{ij} x_i x_j \quad (3)$$

where Y is the response factor, x_i and x_j are the independent variables, and β_0, β_i, β_{ii}, and β_{ij} are the regression coefficients.

Due to a large number of the designed experiments and time-consuming processes of microalgae culture, hydrodynamic and mass transfer studies were performed without microorganisms. Then, to confirm the results, microalgae culture was done under optimum experimental conditions and results were compared with the control experiments.

Table 1. Range and levels of the parameters studied

Variables	Symbols	Real values of coded levels				
		-α	-1	0	+1	+α
Superficial gas velocity (m s^{-1})	V_{gs1}	0.0005	0.0014	0.0037	0.0060	0.0069
Superficial gas velocity (m s^{-1})	V_{gs2}	0.0040	0.0069	0.0139	0.0209	0.0238
Hypotenuse angle (°)	α	10	25	45	65	80

4. RESULTS AND DISCUSSION

According to CCD, twenty experiments were carried out with three factors, each at five levels. The complete experimental design, along with measured responses, is summarized in Table 2. To correlate the factors to the responses, regression models based on Eq. (3) were assessed and the derived equations with their R^2 values (Coefficients of Determination) are presented in Table 3. These equations indicate the influence of the operating variables on each response. The significance of each parameter, which was evaluated by the probability value (p-value), is listed in Table 4. More detailed discussions are given in the following paragraphs.

Table 2. Hydrodynamic and mass transfer responses to the change of three main factors (α, V_{gs1}, and V_{gs2}) according to RSM-designed experiments

No.	Factors			Mass transfer coefficients			Gas holdup			Bubble diameter		Dimensionless time	Power consumption
	α	V_{gs1}	V_{gs2}	k_La_R	k_La_D	k_La_S	ε_R	ε_D	ε_S	d_R	d_D	θ_m	P/V
	(°)	($m.s^{-1}$)		(h^{-1})			(-)			(mm)		(-)	($W.m^{-3}$)
1	45	0.0069	0.0139	20.0	22.0	26.0	0.1654	0.1567	0.1983	4.85	---	0.13	79.34
2	25	0.0014	0.0209	14.5	15.0	14.0	0.1642	0.1485	0.1742	---	6.92	0.77	47.07
3	45	0.0005	0.0139	9.0	13.0	18.0	0.0823	0.0885	0.1014	4.65	6.73	1.27	25.46
4	65	0.0060	0.0069	19.5	24.0	27.0	0.1147	0.1054	0.1369	3.40	6.69	1.06	57.91
5	45	0.0037	0.0139	14.0	15.0	22.0	0.1300	0.1270	0.1578	4.20	5.60	0.85	52.40
6	25	0.0060	0.0069	14.5	14.0	18.5	0.1776	0.1545	0.1799	4.19	7.47	2.08	61.40
7	45	0.0037	0.0139	14.7	14.9	20.5	0.1265	0.1232	0.1559	4.18	5.50	0.84	52.40
8	45	0.0037	0.0238	26.0	17.0	22.0	0.1649	0.1541	0.1976	4.19	6.17	0.29	67.62
9	10	0.0037	0.0139	---	15.9	18.0	---	0.3169	0.3040	3.88	---	---	55.95
10	45	0.0037	0.0139	14.0	16.0	22.0	0.1295	0.1274	0.1583	4.19	5.60	0.85	52.40
11	45	0.0037	0.0139	14.9	15.1	21	0.1295	0.1273	0.1578	4.19	5.6	0.86	52.40
12	25	0.0014	0.0069	12.0	14.0	12.5	0.1152	0.1068	0.1174	4.19	6.43	0.47	28.28
13	65	0.0060	0.0209	23.0	19.3	24.0	0.1420	0.1348	0.1862	4.23	6.62	1.70	75.62
14	80	0.0037	0.0139	21.5	22.0	21.5	0.1235	0.1146	0.1503	4.60	5.79	1.36	50.72
15	65	0.0014	0.0069	13.0	12.3	25.0	0.0691	0.0667	0.0885	5.17	5.81	2.01	26.68
16	45	0.0037	0.0139	15	15.3	21.5	0.1353	0.1333	0.1625	4.21	5.70	0.86	52.40
17	25	0.0060	0.0209	17.5	21.5	20.5	0.2158	0.1890	0.2336	4.19	6.99	2.12	80.18
18	45	0.0037	0.0139	13.5	15	21.5	0.1202	0.1200	0.1501	4.19	5.5	0.86	52.40
19	45	0.0037	0.0040	18.0	14.0	19.0	0.0990	0.0895	0.1022	4.19	5.01	0.75	37.17
20	65	0.0014	0.0209	20.5	8.8	26.0	0.1256	0.1192	0.1510	4.22	5.27	1.87	37.39

Table 3. Final equations of the response surfaces in terms of the actual factors

Response	Predictive equations	R^2
k_La_R	$= +12.81091 + 0.12923 \times \alpha + 1.25040 \times V_{gs1} - 6.40459 \times V_{gs2} + 1.12573 \times V_{gs2}^2$	0.9670
k_La_D	$= +3.0907 + 0.12916 \times \alpha - 0.53343 \times V_{gs1} + 3.29846 \times V_{gs2} + 0.048753 \times \alpha \times V_{gs1} - 0.067437 \times \alpha \times V_{gs2}$	0.9401
k_La_S	$= +4.06975 + 0.29483 \times \alpha + 2.73178 \times V_{gs1} - 0.038852 \times \alpha \times V_{gs1}$	0.8682
ε_R	$= +0.10697 - (3.54646E-3) \times \alpha + 0.025321.V_{gs1} + 0.020399 \times V_{gs2} - (1.61625E-4) \times \alpha \times V_{gs1} - (1.73701E-3) \times V_{gs1} \times V_{gs2} + (3.16465E-5) \times \alpha^2 + (3.16465E-5) \times \alpha^2$	0.9863
ε_D	$= +0.24250 - 7.45953 \times \alpha + (9.74253E-3) \times V_{gs1} + 0.013135 \times V_{gs2} + (6.21996E-5) \times \alpha^2$	0.8859
ε_S	$= +0.19649 - (5.99506E-3) \times \alpha + 0.013958 \times V_{gs1} + (5.09299E-5) \times \alpha^2$	0.8864
t_m	$= -610.96505 + 20.49450 \times \alpha + 190.06425 \times V_{gs1} + 140.40684 \times V_{gs2} - 6.09612 \times \alpha \times V_{gs1} - 2.54045 \times \alpha \times V_{gs2} - 29.77444 \times V_{gs1} \times V_{gs2} - 0.12445 \times \alpha^2$	0.9771
t_C	$= -111.79037 + 4.62685 \times \alpha + 1.68643 \times V_{gs1} + 68.15776 \times V_{gs2} - 0.052903 \times \alpha^2 - 10.46168 \times V_{gs2}^2$	0.9740
P/V	$= +1.34021 - 0.067732 \times \alpha + 8.83612 \times V_{gs1} + 6.50685 \times V_{gs2} - 0.11701 \times \alpha \times V_{gs1} - (8.62890E-3) \times \alpha \times V_{gs2} + (7.50069E-4) \times \alpha^2$	0.9601

k_La_R, k_La_D, and k_La_S: mass transfer coefficient in the riser, downcomer, and separator, respectively. ε_R, ε_D, and ε_S: gas holdup of the riser, downcomer, and separator, respectively. t_m: mixing time. t_C: Circulation time. P/V: Volumetric power consumption

Table 4. ANOVA table for studied responses

Responses	k_La_R	k_La_D	k_La_S	ε_R	ε_D	ε_S	t_m	t_C	P/V
	P values								
Model	<0.0001	0.0005	<0.0001	<0.0001	<0.0001	<0.0001	<0.0001	<0.0001	<0.0001
A	<0.0001	0.0236	<0.0001	<0.0001	<0.0001	<0.0001	<0.0001	0.1433	<0.0001
B	<0.0001	0.0001	0.0029	<0.0001	0.0124	<0.0001	<0.0001	0.0445	<0.0001
C	<0.0001	0.5390	---	<0.0001	0.0100	<0.0001	<0.0001	0.0002	<0.0001
AB	---	0.0303	0.0425	0.0027	---	---	<0.0001	---	<0.0001
AC	---	0.0225	---	---	---	---	<0.0001	---	<0.0001
BC	---	---	---	0.0135	---	---	<0.0001	---	---
A^2	---	---	---	<0.0001	0.0007	0.0004	<0.0001	<0.0001	<0.0001
B^2	---	---	---	---	---	---	<0.0001	---	---
C^2	<0.0001	---	---	---	---	---	<0.0001	<0.0001	---
ABC	---	---	---	---	---	---	<0.0001	---	---
A^2B	---	---	---	---	---	---	<0.0001	---	---
A^2C	---	---	---	---	---	---	<0.0001	---	---
AB^2	---	---	---	---	---	---	<0.0001	---	---
A: superficial gas velocity at the downcomer (V_{gs1}), B: superficial gas velocity at the riser (V_{gs2}), C: hypotenuse angle (α)									

Figure 2 shows θ_m changes versus operating factors. Dimensionless time index, $\theta_m = t_m/t_c$, is the mixing time (t_m) on circulation time (t_c). It is used to eliminate photobioreactor geometry's effects on mixing time and provides suitable criteria to evaluate the mixing process type [29]. If the index is less than one, ($\theta_m < 1$), the radial mixing process is superior to the axial mixing caused by fluid circulation through the reactor. Indeed, the smaller θ_m is, the better the desirable mixing. It can be shown that the desirable fluid mixing was located in the range between 45° and 65° of the hypotenuse angle (intersection of the graphs below the line of θ_m=1), where the lowest value of θ_m was 0.41. At the angles out of this range, the axial mixing due to the fluid circulation was mainly superior to the radial mixing. In other words, when the ratio of the mixing time to the circulation time was 0.41, the best condition of the mixing process was achieved in the photobioreactor.

The response analysis of the mixing time (t_m), the time required to achieve 95 % of the complete mixing [24], indicated that the response (t_m) was significantly influenced by the superficial gas velocities (V_{gs1} and V_{gs2}) and by the angle (α). In the downcomer section, two countercurrent and opposite forces interacted; the upward was due to the gas velocity of V_{gs1} and the downward caused by the liquid weight and gas velocity of V_{gs2}. According to Figures 2a and 2b, at minor angles (10° and 25°), the effect of V_{gs1} increased as a result of photobioreactor height reduction and the reduced liquid weight force. The liquid flow and ascending gas bubbles were coordinated at high V_{gs1} and low V_{gs2} in some cases. This phenomenon caused a sharp increase in the mixing time (Figures 2a and 2b) and system inefficiency. It was observed that the downward forces became stronger gradually with increasing the angle, unlike the opposite (upward) force. Therefore, in the angle range of 45°, optimal mixing was achieved at high V_{gs1} and V_{gs2} values (Figure 2c). The counter forces became equal in the range of 45o to 65o, because the suitable mixing (low t_m) could be obtained both at low V_{gs1} and high V_{gs2} and at high V_{gs1} and low V_{gs2}.

At larger angles, the downward force predominated the opposite one due to the system height increment (Figures 2d and 2e). Therefore, such a system operated as conventional airlift photobioreactors, in which the primary mixing process occurred in the riser section. In this condition, the fluid circulation would be superior to the radial mixing process. Hence, liquid circulation times (t_c) were shorter.

Considering that the fluid circulation rate is adjusted by the gas feeding from the base of the vertical side (V_{gs2}), it could be found that the fluid circulation at low V_{gs1} controlled the process of mixing and stirring. When the liquid mixing time (t_m) was much longer than the circulation time (t_c), significant mixing could be done in the riser section. By increasing V_{gs1} up to 0.0050 m.s^{-1}, in addition to reducing the dependency of t_m on V_{gs2}, V_{gs1} strength was equalized to the total force of V_{gs2} and liquid weight in the hypotenuse. As mentioned earlier, this force caused fluid circulation through the system. In this case, changes in V_{gs2} would not affect mixing time. With a further increase in V_{gs1}, the countercurrent fluid flows in the downcomer section promoted good mixing. Indeed, within the range of V_{gs1} higher than 0.0050 m.s^{-1}, the mixing process was controlled by powerful countercurrent flows created in the downcomer section and the resulted mixing came over the fluid circulation. It was observed that the effect of V_{gs2} on t_m increased again upon exceeding V_{gs1}= 0.0050 m.s^{-1} (Figures 2a-2e). The critical point here is that at the angles of 10° and 25°, the values of t_m were much more extensive than those of t_c (Figures 2a and 2b). Accordingly, significant mixing occurred in the riser and there was not enough time for complete mixing because of the low height of the riser at these angles (especially at 10°). It resulted in an excessive increment of mixing time relative to the circulation time of the fluid.

It should be noted that at three angles of 10°, 25°, and 45°, the relationship between t_m and V_{gs2} at $V_{gs1} < 0.005$ m.s^{-1} was direct and inverse at $V_{gs1} > 0.005$ m.s^{-1}. In other words, at low V_{gs1}, the mixing time increased with increasing V_{gs2} and at high V_{gs1}, increasing V_{gs2} reduced mixing time (improving the mixing process). This relationship was reversed at two angles of 65° and 80°.

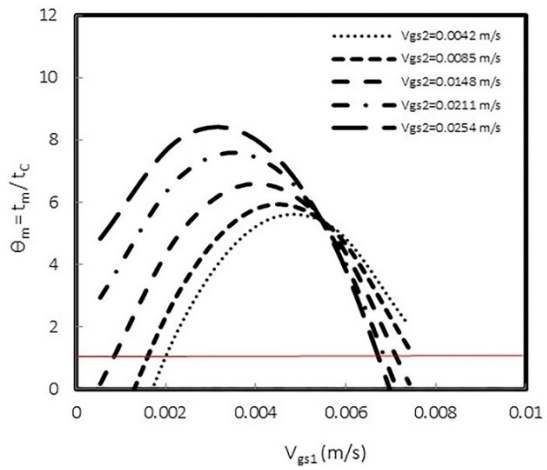

a) α = 10°

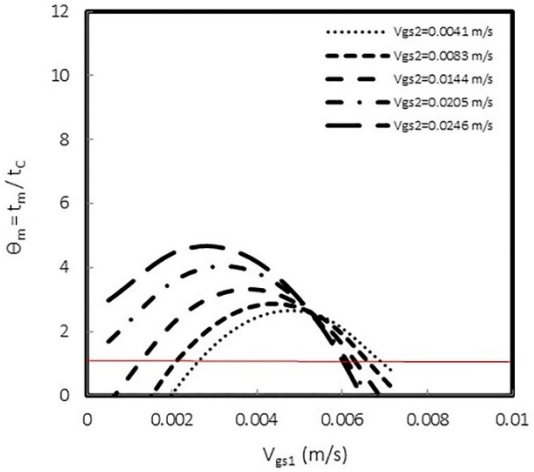

b) α = 25°

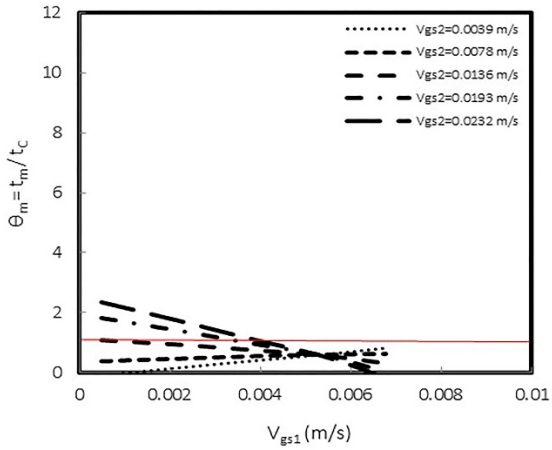

c) α = 45°

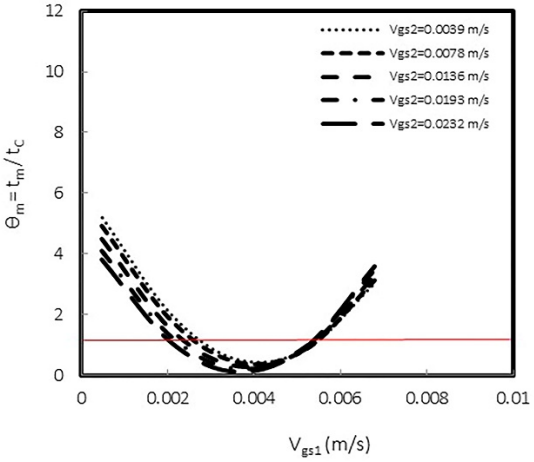

d) α = 65°

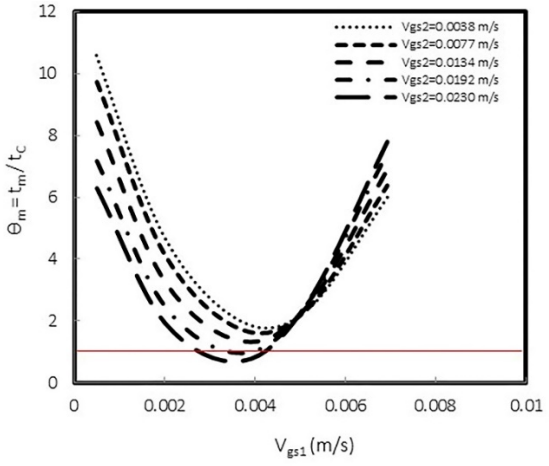

e) α = 80°

Figure 2. Variations of θ_m versus superficial gas velocities (V_{gs1} and V_{gs2}) at different angles

Figure 3 displays the variations of the volumetric mass transfer coefficient (k_La_D) and gas holdup (ε_D) of the downcomer for the superficial gas velocities at different angles. Variation of k_La_D as a function of V_{gs1} was minimal at the angle 10°, despite the positive slope of gas holdup (ε_D). The reason for this phenomenon could be the increase in upcoming bubbles diameter and even in some cases, the conversion of gas flow regime from bubbly to slug flow in the downcomer section due to the V_{gs1} increment.

As shown in Figures 3d and 3e, as the angle increased, the k_La_D changes were incremental at constant V_{gs2}. According to the regression equation for k_La_D exhibited in Table 3, the

angle (α) had a positive effect on k_La_D, linearly, and the interaction with other factors was less significant. Although it was expected that the slope of the k_La_D – V_{gs1} curve decreased or remained at least constant with a slight decrease in gas holdup (ε_D), the increasing slope was observed in this region, unexpectedly. It could be due to the bubbles' diameter decreasing and enhancing the surface area in the downcomer part.

The effects of V_{gs2} on k_La_D had a different trend. Figure 3 shows that increasing the angle from 10° to 80° resulted in reducing the effect of V_{gs2} on k_La_D to an unknown angle (δ) ($45° < \delta < 65°$) where this effect reached zero; and k_La_D just changed under the influence of V_{gs1}. At the angles lower than δ, an increase in V_{gs2} caused the enhancement of the k_La_D, but it was reversed at higher angles. In other words, high mass transfer coefficients could be obtained at lower V_{gs2}. The effect of fluid weight at the angles higher than δ was more considerable among the downward forces in the hypotenuse because of the height increase. Therefore, it is necessary to reduce the power created by the V_{gs2} to keep the balance. If V_{gs2} was raised in this range, t_c decreased while t_m increased. This decline in the mixing rate was the main reason for mass transfer reduction in this bioreactor section. It is worth noting that the highest values of k_La_D at high angles were obtained at high V_{gs1}s and low V_{gs2}s.

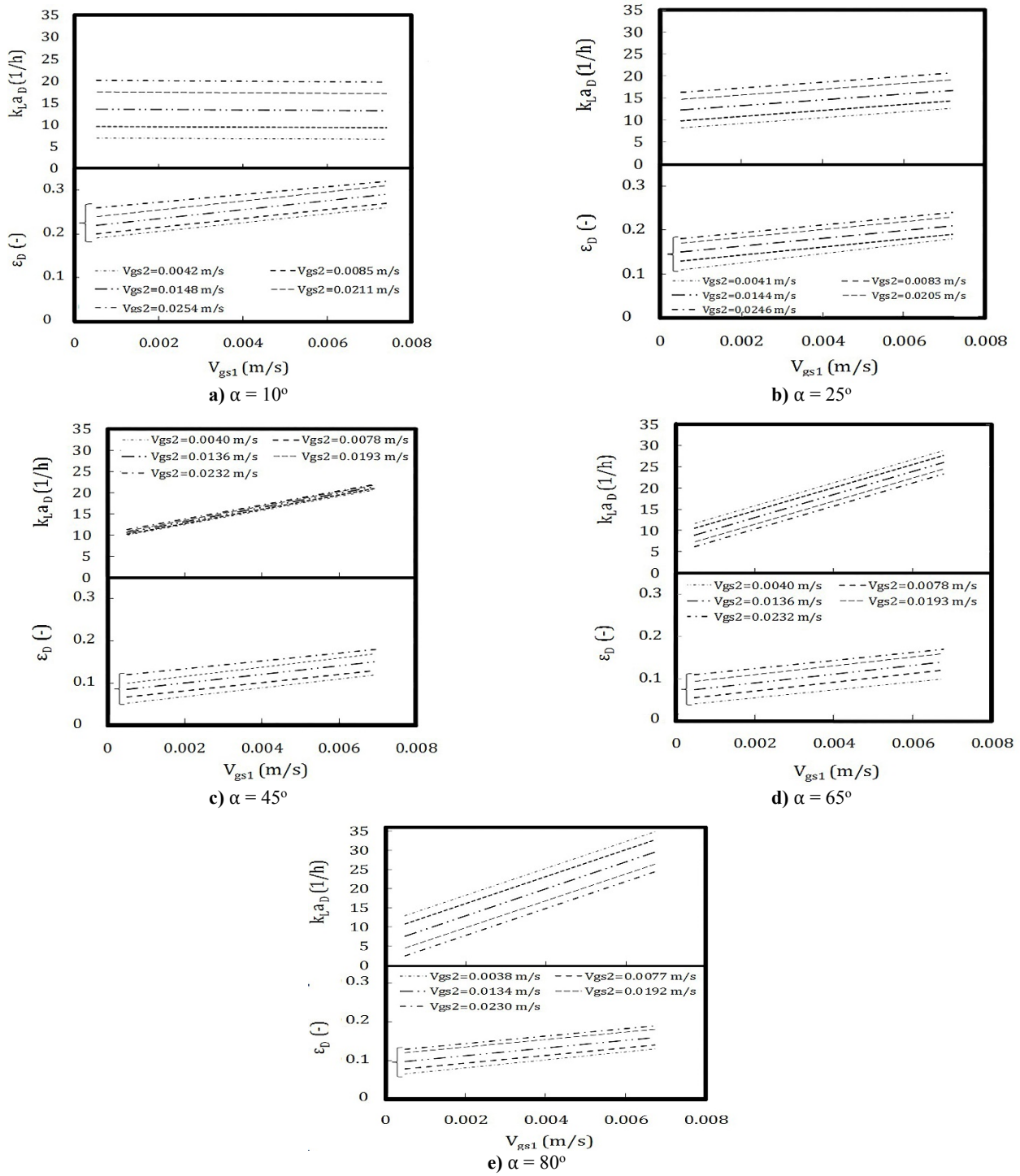

a) α = 10°

b) α = 25°

c) α = 45°

d) α = 65°

e) α = 80°

Figure 3. Changes of k_La_D and ε_D versus superficial gas velocities (V_{gs1} and V_{gs2}) at different angles (α)

Figure 4 presents the variations of the volumetric mass transfer coefficient (k_La_R) and gas holdup (ε_R) of the riser versus three independent factors (V_{gs1}, V_{gs2} and α). As demonstrated, k_La_R had the linear and almost the same relationship (positive effect) with α and V_{gs1} (based on the regression model for k_La_R exhibited in Table 3). Nevertheless, the changes in k_La_R versus V_{gs2} had a different trend (negative in linear and positive in square). Figure 4 confirms that increasing the angle from 10° to an angle (δ) (45° < δ < 65°) reduced the gas holdup in the riser (ε_R). Above this angle, ε_R was almost constant.

Regarding Figures 4a-4e, it was clear that the high amounts of k_La_R could be obtained at the angles above 45°, high V_{gs1}s, and very low or high V_{gs2}s.

Comparison of Figures 3a-3e and 4a-4e shows that the amount of gas holdup in both regions of the riser and downcomer (ε_R and ε_D) was approximately the same and the gas holdup in the riser was just a little more. At the conventional airlift bioreactors, fluid circulation caused by a difference in fluid density has been reported [30]. This difference is caused by relatively uniform distribution of the bubbles in the liquid and is dependent on the gas holdup gradient [31]. Therefore, gas holdup's equivalence leads to the disability of vertical airlift system in fluid circulation, undesirably. However, the geometry of the new bioreactor caused a regular circulation through the system with the minimum difference of gas holdup between the two sections.

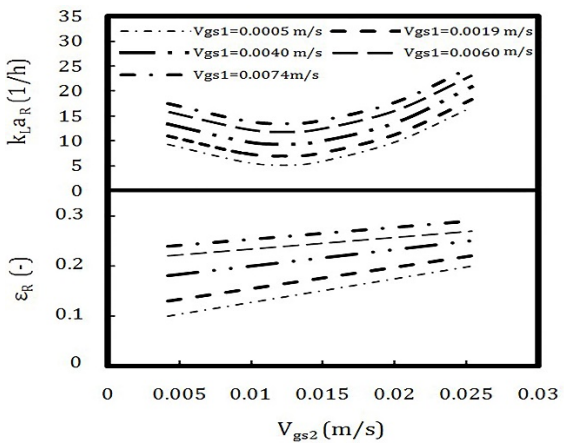

a) α = 10°

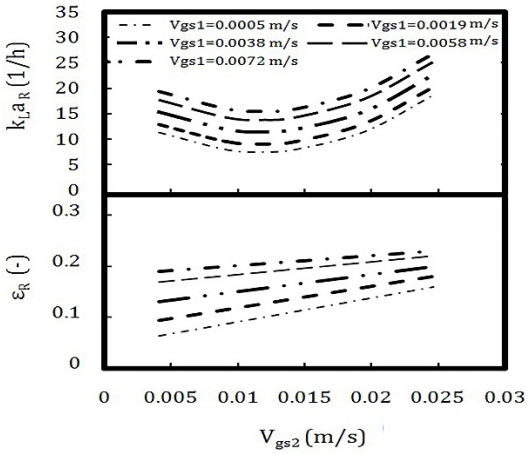

b) α = 25°

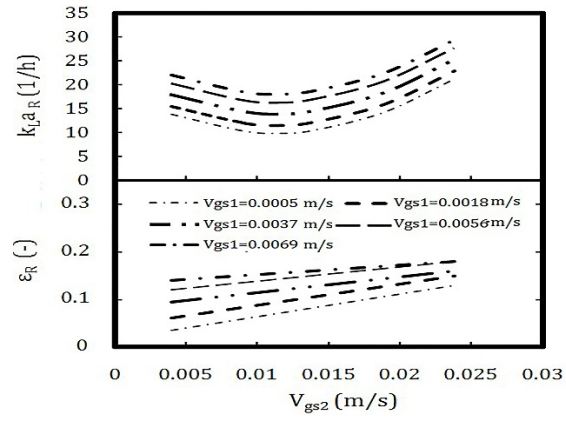

c) α = 45°

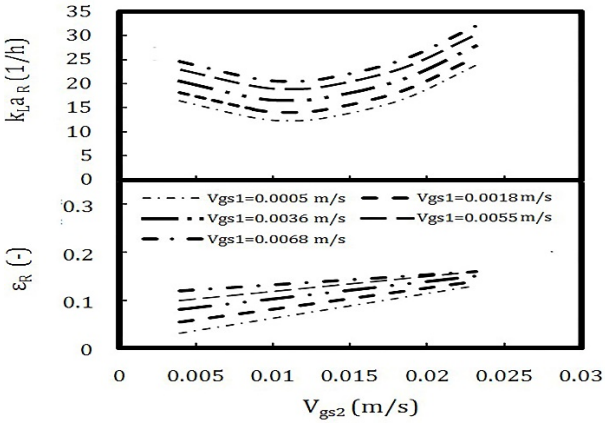

d) α = 65°

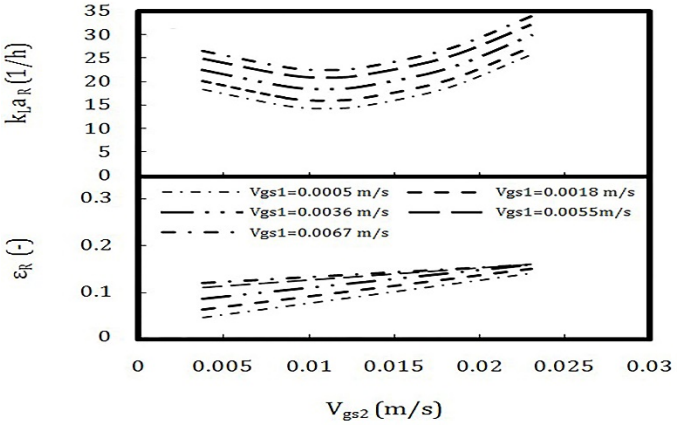

e) α = 80°

Figure 4. Changes of k_La_R and ε_R versus superficial gas velocities (V_{gs1} and V_{gs2}) at different angles (α)

The effect of the three main operating factors on the separator's volumetric mass transfer coefficient (k_La_S) is demonstrated in Figure 5. As shown, k_La_S was strongly affected by two parameters of V_{gs1} and α (see the positive and relatively high coefficients of these two factors in the linear mode of regression model for k_La_S exhibited in Table 3). The influence of V_{gs2} on k_La_S was lower as the k_La difference in the highest and lowest V_{gs2} was just 1.6 h^{-1}. The slope of $k_La_S - V_{gs1}$ curves in the range from 10° to an angle marked as δ (≈ 60°) was always positive (Figures 5a, 5b, and 5c), but at 65° was almost zero (Figure 5d). On the other hand, increasing or decreasing V_{gs1} did not affect the separator's mass transfer amount with the hypotenuse angle of 65°. With a further increase in the angle, the slope became negative (Figure 5e). It means that increasing V_{gs1} would reduce k_La_S. The critical matter in these figures was that the point of V_{gs1}= 0.006 $m.s^{-1}$, which was the only velocity where the k_La_S value was always constant ($k_La_S \approx 25\ h^{-1}$) at all angles. As a result, the maximum values of the k_La_S were observed at high V_{gs1}s and at the angles greater than 45°.

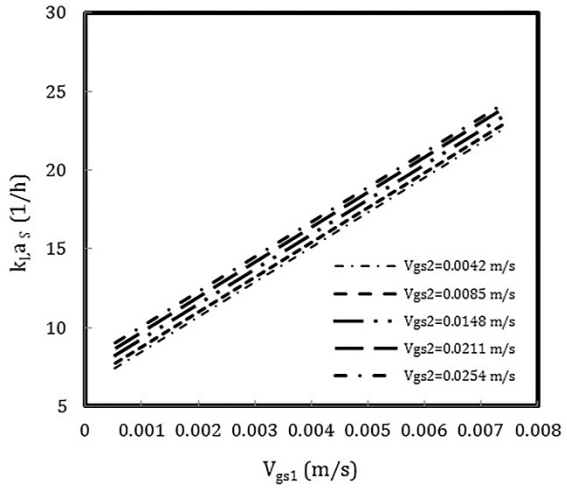

a) α = 10°

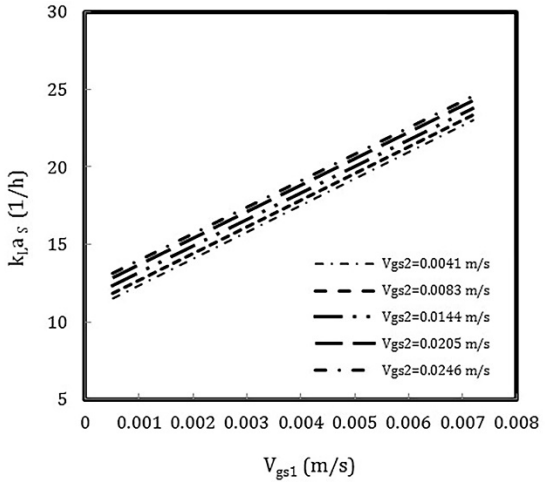

b) α = 25°

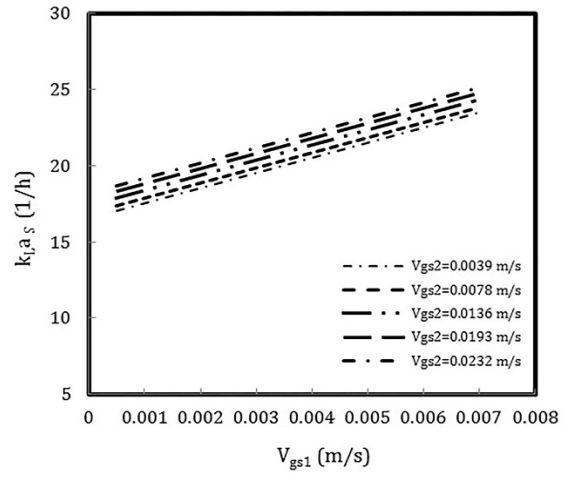

c) α = 45°

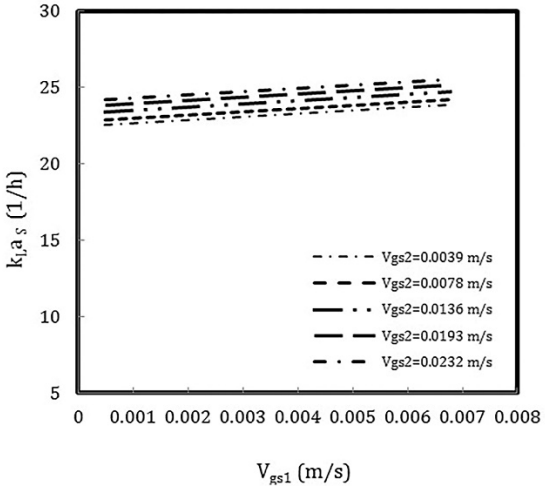

d) α = 65°

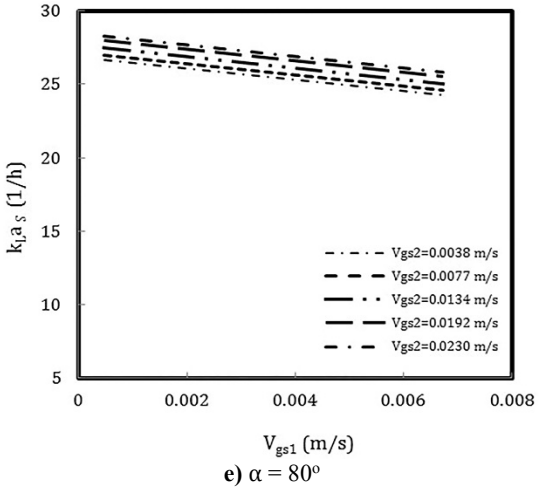

e) α = 80°

Figure 5. Changes of k_La_S versus superficial gas velocities (V_{gs1} and V_{gs2}) at different angles (α)

Figure 6 illustrates the influence of each of three operating variables on a significant characteristic of the system, power consumption per volume (P/V) of the photobioreactor (W/m^3). Accordingly, power consumption variation of the system versus angle was not considerable, and increasing the angle led to an insignificant reduction in it. However, this characteristic was strongly influenced by superficial gas velocities, V_{gs2} and especially V_{gs1}. A linear power consumption increment could be observed upon increase in the velocities. An increase in V_{gs1} raised power consumption and led to a significant increase in k_La_D and k_La_R [see Figures 3 and 4]. As previously mentioned, increasing V_{gs2} could have a positive influence on the volumetric mass transfer coefficient in the riser (k_La_R) and, in addition to power consumption increment, mainly decreased k_La_D. Despite the insignificant effect of the hypotenuse angle (α) on power consumption, the mass transfer coefficients in both riser and downcomer represented high sensitivity. Therefore, by optimizing the photobioreactor's operating conditions, the maximum mass transfer and mixing rates could be achieved along with the minimum power consumption in the system.

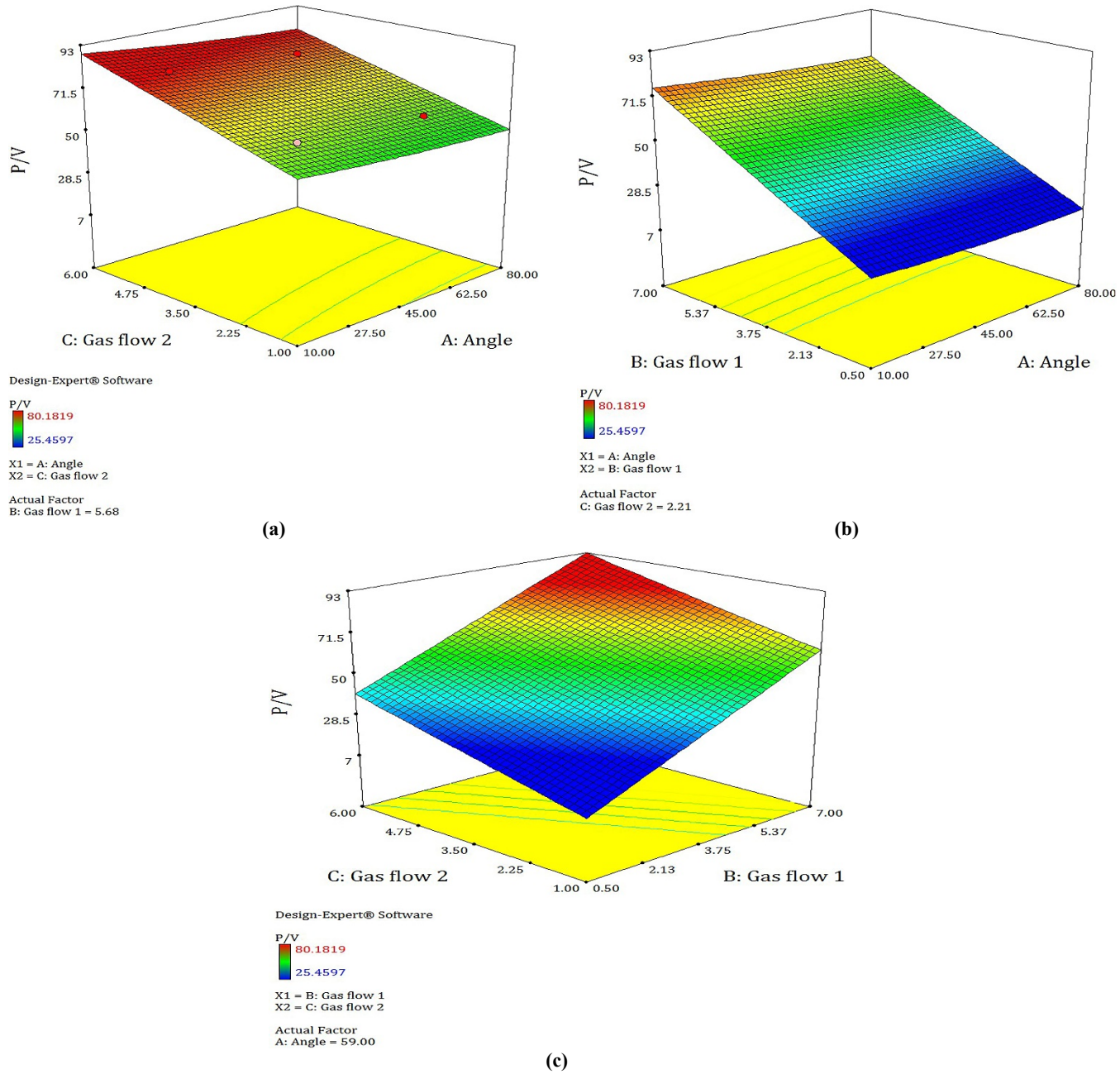

Figure 6. Power consumption of the photobioreactor at (a) different gas flows 2 (V_{gs2}) and the angle (α); (b) different gas flows 1 (V_{gs1}) and the angle (α); (c) different gas flows 1 (V_{gs1}) and gas flow 2 (V_{gs2})

As mentioned before, the designed experiments' desirable goal was to reach the maximum mass transfer in the shortest mixing time and minimum power consumption, simultaneously. Regarding the analysis, the downcomer's counter forces were identical at the superficial gas velocity of V_{gs1} = 0.0050 $m.s^{-1}$, where θ_m did not change by V_{gs2} variations. Besides, the $\theta_m - V_{gs1}$ curve at different V_{gs2}s was mainly located in the range of the dimensionless time less than one ($\theta_m < 1$) at an angle of $\delta \approx 60^o$. It means that the mixing time was lower than the circulation time, and the optimum mixing process could be observed in the shortest amount of time.

Also, maximum effective mass transfer was located at large values of V_{gs1} and small amounts of V_{gs2} and the angles higher than 45°. On the other hand, the upper limit of the optimum angle could not exceed 65° to achieve the minimum value of θ_m. It should reduce the superficial gas velocities as much as possible to minimize power consumption. Since the excessive reduction of V_{gs1} had a little adverse effect on the volumetric mass transfer coefficient in the separator ($k_L a_S$), power consumption saving could be achieved by reducing V_{gs2}. As a result, the geometry of the studied photobioreactor had better mass transfer than other configurations. This was caused by better mixing (decreased mixing time) as a result of countercurrent flow in the downcomer when power consumption slightly increased [32].

According to the analysis, each independent variable's influences and limitations to attain the desired goal, the optimum conditions, and the actual and predicted responses are listed in Table 5. The optimal conditions provided by the software were determined as follows: V_{gs1} = 0.0050 m.s^{-1}, V_{gs2} = 0.0080 m.s^{-1}, and α = 59 ~ 60°. The empirical experiments were conducted in optimal conditions to confirm the RSM predictions, and the responses were also measured practically. According to Table 5, there is acceptable consistency between predicted values and experimental results.

4.1. Confirmation of the optimal conditions with microalgae culture

The microorganism's culture at the optimum angle (60°) was performed to confirm the findings and was compared with two angles of 10° and 80° as control conditions. For this purpose, the microalgae growth rate was obtained by dry biomass weight measurements [33]. The same conditions were assigned for the culture medium, considering the operating parameters like temperature, pH, inoculation time, and concentration. As shown in Figure 7, there was a significant difference in the growth rate of *Chlorella vulgaris* at the angle of 60° compared to 10° and 80°. It was confirmed that the optimal mixing rate was a very effective agent in the cultivating process. Increasing the mixing rate improved the accessibility of the nutrients and CO_2. Also, by removing the downcomer's dark zone, the tube center developed the appropriate culture media for microorganisms. Additionally, the growth curves confirmed the optimum conditions and indicated the high impact of the hydrodynamic tensions on the culture. Furthermore, it was found that the maximum concentration of biomass (X_{max}=1.4 g.l^{-1}) was achieved faster (11th day of cultivation) than similar studies [34]. The obtained conditions were compared with some similar studies, as shown in Table 6. These results have drawn much more attention to the significance of the airlift photobioreactors' geometry and design to produce microalgae efficiently.

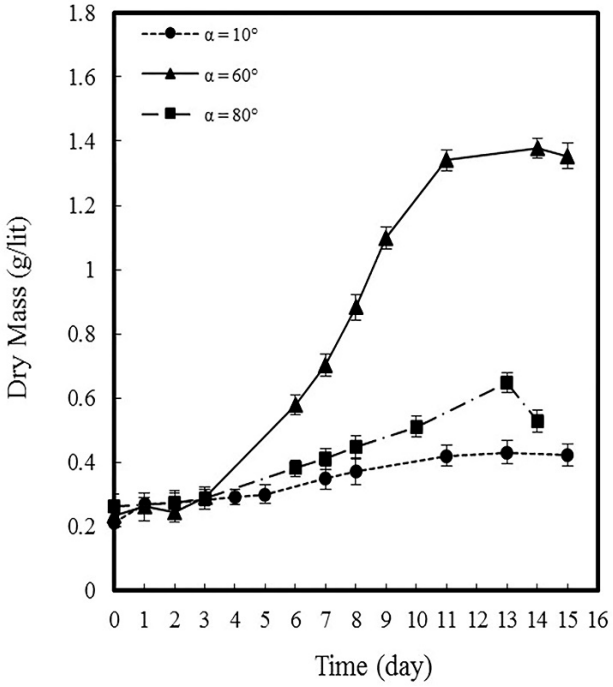

Figure 7. Growth curve of *Chlorella vulgaris* at angles of 10°, 60°, and 80° obtained by dry mass measurement

Table 6. Comparison of growth factors of *Chlorella vulgaris* in photobioreactors of different studies

Reference	Growth factors				Comments
	μ_{max} (day^{-1})	X_{max} (g.L^{-1})	P_{max} (g.L^{-1}.day^{-1})	t_d (day)	
This work	0.214	1.379	0.100	3.200	Carbon source: air, system type: external loop airlift photobioreactor.
[34]	0.130	1.220	0.100		Carbon source: CO_2
[35]	0.205	0.590	---		Carbon source: air, system type: CSTR, operating volume: 10 L.
[36]	---	---	0.100		Carbon source: CO_2
[37]	---	---	0.200		Carbon source: CO_2, system type: 250 ml flask
[38]	---	---	0.010		Carbon source: CO_2, system type: mixed tank, operating volume: 2 L
[39]	---	---	0.020-0.040		Carbon source: CO_2
[40]	---	---	0.030-0.040		Carbon source: CO_2
μ_{max}: maximum specific growth rate, X_{max}: maximum biomass concentration, P_{max}: maximum biomass productivity, t_d: doubling time					

5. CONCLUSIONS

The optimization process of a triangular external loop airlift PBR was performed by the RSM to maximize the volumetric mass transfer coefficients (k_La) and minimize the power consumption per volume (P/V) as well as the mixing time (t_m) as responses. The effects of the three main factors, superficial gas velocities (V_{gs1} and V_{gs2}), and the hypotenuse angle (α) on the system performance were investigated. The optimal values were obtained as follows α = 59°, V_{gs1} = 0.0050 m.s^{-1}, and V_{gs2} = 0.008 m.s^{-1}. It was also found that the V_{gs1} and α were the most effective factors in hydrodynamic and mass transfer behavior of the system. The sensitivity of all responses to V_{gs1} was high and of almost equal importance. However, despite the great influence of α on the mixing and mass transfer, it had less impact on power consumption. Moreover, V_{gs2} variations possessed a considerable effect on the riser's mass transfer coefficient and power consumption and made fewer mixing time changes. Predictive, second-order mathematical models were presented to correlate the individual parameters to the responses with high R^2 ranging from 0.88 to 0.96. Also, mathematical models were confirmed by comparison of the actual and predicted response values.

The dimensionless time (θ_m) was 0.41 under optimum conditions. θ_m less than one ($\theta_m < 1$) was the cause for improving the mixing process due to the fluid's radial distribution rather than its axial circulation. Finally, growth curves of the *Chlorella vulgaris* verified the optimum condition, practically and demonstrated higher biomass concentration and shorter culture duration than those in other studies.

6. ACKNOWLEDGEMENT

The authors would like to gratefully acknowledge the Biotechnology Group, Faculty of Chemical Engineering, Tarbiat Modares University for their support.

REFERENCES

1. Tagliaferro, G.V., Izário Filho, H.J., Chandel, A.K., da Silva, S.S., Silva, M.B. and dos Santos, J.C., "Continuous cultivation of *Chlorella minutissima 26a* in a tube-cylinder internal-loop airlift photobioreactor to support 3G biorefineries", ***Renewable Energy***, Vol. 130, (2019), 439-445. (https://doi.org/10.1016/j.renene.2018.06.041).
2. Carvalho, A.P., Meireles, L.A. and Malcata, F.X., "Microalgal reactors: A review of enclosed system designs and performances", ***Biotechnology Progress***, Vol. 22, No. 6, (2006), 1490-1506. (https://doi.org/10.1021/bp060065r).
3. Essadki, A., Bennajah, M., Gourich, B., Vial, C., Azzi, M. and Delmas, H., "Electrocoagulation/electroflotation in an external-loop airlift reactor—Application to the decolorization of textile dye wastewater: A case study", ***Chemical Engineering and Processing: Process Intensification***, Vol. 47, No. 8, (2008), 1211-1223. (https://doi.org/10.1016/j.cep.2007.03.013).
4. Choi, K.H., "Hydrodynamic and mass transfer characteristics of external-loop airlift reactors without an extension tube above the downcomer", ***Korean Journal of Chemical Engineering***, Vol. 18, No. 2, (2001), 240-246. (https://doi.org/10.1007/BF02698466).
5. Nikakhtari, H. and Hill, G.A., "Continuous bioremediation of phenol-polluted air in an external loop airlift bioreactor with a packed bed", ***Journal of Chemical Technology & Biotechnology: International Research in Process, Environmental & Clean Technology***, Vol. 81, No. 6, (2006), 1029-1038. (https://doi.org/10.1002/jctb.1520).
6. Bahadar, A. and Khan, M.B., "Progress in energy from microalgae: A review", ***Renewable and Sustainable Energy Reviews***, Vol. 27, (2013), 128-148. (https://doi.org/10.1016/j.rser.2013.06.029).
7. Barbosa, M.J., Janssen, M., Ham, N., Tramper, J. and Wijffels, R.H., "Microalgae cultivation in air-lift reactors: Modeling biomass yield and growth rate as a function of mixing frequency", ***Biotechnology and Bioengineering***, Vol. 82, No. 2, (2003), 170-179. (https://doi.org/10.1002/bit.10563).
8. Zeng, X., Danquah, M.K., Chen, X.D. and Lu, Y., "Microalgae bioengineering: From CO_2 fixation to biofuel production", ***Renewable and Sustainable Energy Reviews***, Vol. 15, No. 6, (2011), 3252-3260. (https://doi.org/10.1016/j.rser.2011.04.014).
9. Scarsella, M., Torzillo, G., Cicci, A., Belotti, G., De Filippis, P. and Bravi, M., "Mechanical stress tolerance of two microalgae", ***Process Biochemistry***, Vol. 47, No. 11, (2012), 1603-1611. (https://doi.org/10.1016/j.procbio.2011.07.002).
10. Powtongsook, S., Kaewpintong, K., Shotipruk, A. and Pavasant, P., "Effect of superficial gas velocity on growth of the green microalga haematococcus pluvialis in airlift photobioreactor", Studies in surface science and catalysis, Elsevier, (2006),.481-484. (https://doi.org/10.1016/S0167-2991(06)81638-1).
11. Hoseinkhani, N., Jalili, H., Ansari, S. and Amrane, A., "Impact of bubble size on docosahexaenoic acid production by *Crypthecodinium cohnii* in bubble column bioreactor", ***Biomass Conversion and Biorefinery***, Vol. 11, (2019), 1137-1144. (https://doi.org/10.1007/s13399-019-00510-5).
12. Ugwu, C., Aoyagi, H. and Uchiyama, H., "Photobioreactors for mass cultivation of algae", ***Bioresource Technology***, Vol. 99, No. 10, (2008), 4021-4028. (https://doi.org/10.1016/j.biortech.2007.01.046).
13. Barahoei, M., Hatamipour, M.S. and Afsharzadeh, S., "CO_2 capturing by *Chlorella vulgaris* in a bubble column photo-bioreactor; Effect of bubble size on CO_2 removal and growth rate", ***Journal of CO_2 Utilization***, Vol. 37, (2020), 9-19. (https://doi.org/10.1016/j.jcou.2019.11.023).
14. Geng, S., Li, Z., Liu, H., Yang, C., Gao, F., He, T. and Huang, Q., "Hydrodynamics and mass transfer in a slurry external airlift loop reactor integrating mixing and separation", ***Chemical Engineering Science***, Vol. 211, (2020), 115294. (https://doi.org/10.1016/j.ces.2019.115294).
15. Zhang, L., Wu, M., Han, Y., Liu, M. and Niu, J., "Structural parameter optimization for novel internal-loop iron–carbon micro-electrolysis reactors using computational fluid dynamics", ***Chinese Journal of Chemical Engineering***, Vol. 27, No. 4, (2019), 737-744. (https://doi.org/10.1016/j.cjche.2018.08.001).
16. Reyna-Velarde, R., Cristiani-Urbina, E., Hernández-Melchor, D.J., Thalasso, F. and Cañizares-Villanueva, R.O., "Hydrodynamic and mass transfer characterization of a flat-panel airlift photobioreactor with high light path", ***Chemical Engineering and Processing: Process Intensification***, Vol. 49, No. 1, (2010), 97-103. (https://doi.org/10.1016/j.cep.2009.11.014).
17. Fadavi, A. and Chisti, Y., "Gas holdup and mixing characteristics of a novel forced circulation loop reactor", ***Chemical Engineering Journal***, Vol. 131, No. 1-3, (2007), 105-111. (https://doi.org/10.1016/j.cej.2006.12.037).
18. Yazdian, F., Hajiabbas, M.P., Shojaosadati, S.A., Nosrati, M., Vasheghani-Farahani, E. and Mehrnia, M., "Study of hydrodynamics, mass transfer, energy consumption, and biomass production from natural gas in a forced-liquid vertical tubular loop bioreactor", ***Biochemical Engineering Journal***, Vol. 49, No. 2, (2010), 192-200. (https://doi.org/10.1016/j.bej.2009.12.013).
19. Yazdian, F., Shojaosadati, S.A., Nosrati, M., Mehrnia, M. and Vasheghani-Farahani, E., "Study of geometry and operational conditions on mixing time, gas hold up, mass transfer, flow regime and biomass production from natural gas in a horizontal tubular loop bioreactor", ***Chemical Engineering Science***, Vol. 64, No. 3, (2009), 540-547. (https://doi.org/10.1016/j.ces.2008.09.031).
20. Gao, X., Kong, B. and Vigil, R.D., "Multiphysics simulation of algal growth in an airlift photobioreactor: Effects of fluid mixing and shear stress", ***Bioresource Technology***, Vol. 251, (2018), 75-83. (https://doi.org/10.1016/j.biortech.2017.12.014).
21. Chiu, S.Y., Tsai, M.T., Kao, C.Y., Ong, S.C. and Lin, C.S., "The air-lift photobioreactors with flow patterning for high-density cultures of microalgae and carbon dioxide removal", ***Engineering in Life Sciences***, Vol. 9, No. 3, (2009), 254-260. (https://doi.org/10.1002/elsc.200800113).
22. Lakaniemi, A.M., Intihar, V.M., Tuovinen, O.H. and Puhakka, J.A., "Growth of *Chlorella vulgaris* and associated bacteria in

photobioreactors", ***Microbial Biotechnology***, Vol. 5, No. 1, (2012), 69-78. (https://doi.org/10.1111/j.1751-7915.2011.00298.x).

23. Posten, C., "Design principles of photo-bioreactors for cultivation of microalgae", ***Engineering in Life Sciences***, Vol. 9, No. 3, (2009), 165-177. (https://doi.org/10.1002/elsc.200900003).
24. Mendoza, J., Granados, M., De Godos, I., Acién, F., Molina, E., Banks, C. and Heaven, S., "Fluid-dynamic characterization of real-scale raceway reactors for microalgae production", ***Biomass and Bioenergy***, Vol. 54, (2013), 267-275. (https://doi.org/10.1016/j.biombioe.2013.03.017).
25. Verlaan, P., Van Eijs, A., Tramper, J., Van't Riet, K. and Luyben, K.C.A., "Estimation of axial dispersion in individual sections of an airlift-loop reactor", ***Chemical Engineering Science***, Vol. 44, No. 5, (1989), 1139-1146. (https://doi.org/10.1016/0009-2509(89)87013-7).
26. Shadpoor, S., Pirouzi, A., Hamze, H. and Mazaheri, D., "Determination of bodenstein number and axial dispersion of a triangular external loop airlift reactor", ***Chemical Engineering Research and Design***, Vol. 165, (2021), 61-68. (https://doi.org/10.1016/j.cherd.2020.10.018).
27. Guo, X., Yao, L. and Huang, Q., "Aeration and mass transfer optimization in a rectangular airlift loop photobioreactor for the production of microalgae", ***Bioresource tTechnology***, Vol. 190, (2015), 189-195. (https://doi.org/10.1016/j.biortech.2015.04.077).
28. Kochem, L.H., Da Fré, N.C., Redaelli, C., Rech, R. and Marcílio, N.R., "Characterization of a novel flat-panel airlift photobioreactor with an internal heat exchanger", ***Chemical Engineering & Technology***, Vol. 37, No. 1, (2014), 59-64. (https://doi.org/10.1002/ceat.201300420).
29. Mirón, A.S., García, M.-C.C., Camacho, F.G., Grima, E.M. and Chisti, Y., "Mixing in bubble column and airlift reactors", ***Chemical Engineering Research and Design***, Vol. 82, No. 10, (2004), 1367-1374. (https://doi.org/10.1205/cerd.82.10.1367.46742).
30. Vunjak-Novakovic, G., Kim, Y., Wu, X., Berzin, I. and Merchuk, J.C., "Air-lift bioreactors for algal growth on flue gas: Mathematical modeling and pilot-plant studies", ***Industrial & Engineering Chemistry Research***, Vol. 44, No. 16, (2005), 6154-6163. (https://doi.org/10.1021/ie049099z).
31. Reilly, I., Scott, D., Debruijn, T. and MacIntyre, D., "The role of gas phase momentum in determining gas holdup and hydrodynamic flow regimes in bubble column operations", ***The Canadian Journal of Chemical Engineering***, Vol. 72, No. 1, (1994), 3-12. (https://doi.org/10.1002/cjce.5450720102).
32. Pirouzi, A., Nosrati, M., Shojaosadati, S.A. and Shakhesi, S., "Improvement of mixing time, mass transfer, and power consumption in an external loop airlift photobioreactor for microalgae cultures", ***Biochemical Engineering Journal***, Vol. 87, (2014), 25-32. (https://doi.org/10.1016/j.bej.2014.03.012).
33. Roselet, F., Vandamme, D., Roselet, M., Muylaert, K. and Abreu, P.C., "Screening of commercial natural and synthetic cationic polymers for flocculation of freshwater and marine microalgae and effects of molecular weight and charge density", ***Algal Research***, Vol. 10, (2015), 183-188. (https://doi.org/10.1016/j.algal.2015.05.008).
34. Abreu, A.P., Fernandes, B., Vicente, A.A., Teixeira, J. and Dragone, G., "Mixotrophic cultivation of *Chlorella vulgaris* using industrial dairy waste as organic carbon source", ***Bioresource Technology***, Vol. 118, (2012), 61-66. (https://doi.org/10.1016/j.biortech.2012.05.055).
35. Sacasa Castellanos, C., "Batch and continuous studies of *Chlorella vulgaris* in photo-bioreactors", Electronic Thesis and Dissertation Repository, (2013), 1113. (https://ir.lib.uwo.ca/etd/1113).
36. Yoo, C., Jun, S.-Y., Lee, J.-Y., Ahn, C.-Y. and Oh, H.-M., "Selection of microalgae for lipid production under high levels carbon dioxide", ***Bioresource Technology***, Vol. 101, No. 1, (2010), S71-S74. (https://doi.org/10.1016/j.biortech.2009.03.030).
37. Rodolfi, L., Chini Zittelli, G., Bassi, N., Padovani, G., Biondi, N., Bonini, G. and Tredici, M.R., "Microalgae for oil: Strain selection, induction of lipid synthesis and outdoor mass cultivation in a low-cost photobioreactor", ***Biotechnology and Bioengineering***, Vol. 102, No. 1, (2009), 100-112. (https://doi.org/10.1002/bit.22033).
38. Liang, Y., Sarkany, N. and Cui, Y., "Biomass and lipid productivities of *Chlorella vulgaris* under autotrophic, heterotrophic and mixotrophic growth conditions", ***Biotechnology Letters***, Vol. 31, No. 7, (2009), 1043-1049. (https://doi.org/10.1007/s10529-009-9975-7).
39. Scragg, A., Illman, A., Carden, A. and Shales, S., "Growth of microalgae with increased calorific values in a tubular bioreactor", ***Biomass and Bioenergy***, Vol. 23, No. 1, (2002), 67-73. (https://doi.org/10.1016/S0961-9534(02)00028-4).
40. Illman, A., Scragg, A. and Shales, S., "Increase in Chlorella strains calorific values when grown in low nitrogen medium", ***Enzyme and Microbial Technology***, Vol. 27, No. 8, (2000), 631-635. (https://doi.org/10.1016/S0141-0229(00)00266-0).